Charge localization and fragmentation dynamics of ionized helium clusters

M. Ovchinnikov, B. L. Grigorenko,[a] K. C. Janda, and V. A. Apkarian
Department of Chemistry, University of California, Irvine, California 92697-2025

(Received 9 February 1998; accepted 6 March 1998)

The dynamics of He_n^+, $n=3-13$, clusters formed by electron impact ionization of the neutral is studied theoretically using mixed quantum/classical dynamics by both mean-field and surface hopping methods. Potential energy surfaces and nonadiabatic couplings among them are determined from a semiempirical, minimal basis DIM Hamiltonian. The dynamics of hole hopping, hole localization, and cluster fragmentation are described through trajectory data. He_3^+ clusters, with initial conditions given by the zero-energy quantum distribution of nuclear coordinates, dissociate through two-channels, $He+He+He^+$ and $He+He_2^+$ with relative yields of 20% and 80%. The motif of hole localization on a pair of atoms, and subsequent dissociation of the initial pair with hole hop to a new pair is observed in trimers, and repeats in larger clusters. In the larger clusters, hole hopping among He_2 pairs provides an additional, less important mechanism of charge migration. The coupled electronic-nuclear dynamics of triatomic units describes the mechanism of energy loss, by transfer of vibrational to translational energy. This leads to ejection of energetic neutral atoms as well as the ejection of He_2^+ prior to evaporative cooling of the cluster. He_2^+ is the exclusive charged unit produced in the fragmentation of He_{13}^+ clusters. In bulk He the same dynamics should lead to fast vibrational relaxation $t<10$ ps and formation of He_3^+ as the positive ion core. © *1998 American Institute of Physics.* [S0021-9606(98)02122-9]

I. INTRODUCTION

Spectroscopy and dynamics in neat and doped helium clusters is an active field of research at present.[1] This activity is propelled by a variety of motivations, the understanding of superfluidity at the molecular level being one.[1,2] For a rather complete review of the field we refer to the recent review article by Whalley.[1] Mass spectrometry is one of the more common tools for the characterization of clusters, and has been used incisively in the case of He clusters, from the smallest units such as He_2^+,[3] and He_3^+,[4,5] to large superfluid He droplets.[2,5–14] Given the very week binding energy of He clusters, extensive fragmentation ensues upon ionization. The observed fragmentation patterns have been used to reconstruct the dynamics of charge transfer and localization, and the likely paths of energy dissipation that lead to the formation of various ionic and neutral fragments.[9–14] The fundamental issues raised in these studies, namely, the physics of hole hopping, self-trapping, and the nature of self-trapped holes, also arise in the case of bulk liquid helium.[15] Based on drift velocity measurements,[16] it is known that the self-trapped hole has a very large effective mass in superfluid He, and it is recognized that the central positive charge must create a large local density (''snowball'') around it.[15] Yet the exact nature of the central ion and the mechanism of its formation and relaxation are not well understood. The interrogation of these processes in real time are now accessible to experiments, where it has been shown that using ultrafast lasers the ions can be gently, and suddenly generated in the bulk.[17] In this paper, we provide mixed quantum classical simulations of nonadiabatic dynamics that follows the sudden ionization of He_n^+ ($n=3-13$) clusters. The description of the coupled motion of hole and nuclear coordinates may help elucidate the validity of assumptions made in estimating time scales of hole hopping and localization and therefore implied ranges of charge migration, and subsequent fragmentation in the case of clusters. We relate the results to experimental data on small clusters, and comment on implications regarding dynamics in the bulk.

Due to the light mass of He atoms and the very weak van der Waals interaction between He atoms, He clusters are strictly quantum in nature.[1] While the He–He potential is bound by only $8\ cm^{-1}$,[18–21] the He_2^+ ion is bound by $20\,000\ cm^{-1}$.[22–25] Accordingly, the Hamiltonian of a small He_n^+ cluster is dominated by the $He–He^+$ potential. As such, to a good approximation, it is possible to describe the dynamics of the ionized cluster by mixed quantum-classical simulations, where the motion of the hole is followed by solving the time dependent Schrödinger equation, while the nuclei move classically under the Ehrenfest force exerted by the hole. Thus, the methodology we use is very similar to that used in the description of dynamics in the more classical cluster ions,[26–28] such as Ar_n^+ ions.[28] We also use the semiempirical diatomics-in-molecules (DIM) formalism to describe the interactions within the ionized cluster.[26–30] The quantum nature of the precursor neutral cluster only arises in considerations of the initial distribution of nuclear coordinates, and for that, guidance is provided by the quantum Monte Carlo calculations of structures of neutral He clusters.[31–33] The description of the initial electronic wave function, i.e., the description of the hole created by electron impact ionization, can be expected to vary as a function of

[a]Permanent address: Department of Chemistry, Moscow State University, Moscow, 119899, Russian Federation.

cluster size. In the simulations, we assume that electron impact ionization puts the charge on a single atom. The alternative choice would be the creation of a hole in one of the vertically accessible adiabatic states of the conduction band, where the hole function would be delocalized over the cluster. In the small clusters considered here, this initial choice does nor effect the subsequent dynamics to any significant extent. Due to the large and uniform distribution of interatomic distances in the neutral cluster, the atomic hole delocalizes before any significant nuclear motion occurs. Nuclear motion, which breaks the cluster symmetry, leads to localization and self-trapping of the hole, as we describe in some detail.

In what follows, in Sec. II we describe the construct of the DIM Hamiltonian used in the simulations; in Sec. III we describe the algorithms used for the computation of the nonadiabatic dynamics, a recent general review of which has been given by Coker.[34] We use mean-field simulations to establish time scales of the initial dynamics, and use the surface hopping method of Tully to ascertain final channels.[35] The results of these simulations are presented and discussed in Sec. IV, and general conclusions are drawn in Sec. V.

II. POTENTIAL ENERGY SURFACES

The electronic Hamiltonian is constructed based on the DIM approach, where the polyatomic Hamiltonian is expressed in terms of atomic and diatomic functions,[36–38]

$$\hat{H}=\sum_{a<b}\hat{H}_{ab}-(n-2)\sum_{a}\hat{H}_{a}. \tag{1}$$

Here, the polyatomic basis set consists of n functions ϕ_i, $i=1,...,n$ corresponding to the charge localized on atom i. We set the atomic Hamiltonians to zero, which is equivalent to setting the origin of potential energy to the dissociation limit consisting of $n-1$ neutral He atoms and one He^+ ion at infinite internuclear separation. The components of the diatomic Hamiltonians are restricted to

$$(H_{ab})_{ij}=\langle\phi_i|H_{ab}|\phi_j\rangle=\begin{cases}\frac{1}{2}\left(V_{\Sigma_g(He_2^+)}(r_{ab})+V_{\Sigma_u(He_2^+)}(r_{ab})\right) & \text{if } i=a=j \text{ or } i=b=j\\ \frac{1}{2}\left(V_{\Sigma_g(He_2^+)}(r_{ab})-V_{\Sigma_u(He_2^+)}(r_{ab})\right) & \text{if } i=a\neq j,\ i=b\neq j,\ j=a\neq i \text{ or } j=b\neq i\\ V_{\Sigma(He_2)}(r_{ab}) & \text{if } i=j\neq a,b\\ 0 & \text{otherwise}\end{cases} \tag{2}$$

which implies restricting the atomic bases to single $^1S_0$ states on both He^+ and He. For the He_3^+ cluster, the 1–2 fragment Hamiltonian is given explicitly as

$$H_{12}=\begin{pmatrix}\frac{1}{2}\left(V_{\Sigma_g(He_2^+)}(r_{12})+V_{\Sigma_u(He_2^+)}(r_{12})\right) & \frac{1}{2}\left(V_{\Sigma_g(He_2^+)}(r_{12})-V_{\Sigma_u(He_2^+)}(r_{12})\right) & 0\\ \frac{1}{2}\left(V_{\Sigma_g(He_2)}(r_{12})-V_{\Sigma_u(He_2^+)}(r_{12})\right) & \frac{1}{2}\left(V_{\Sigma_g(He_2^+)}(r_{12})+V_{\Sigma_u(He_2^+)}(r_{12})\right) & 0\\ 0 & 0 & V_{\Sigma(He_2)}(r_{12})\end{pmatrix} \tag{3}$$

and the addition of the three fragments, H_{12}, H_{23}, H_{13}, yields the total Hamiltonian in Eq. (1).

This DIM construct with atomic bases limited to $^1S_0$ states has already been reported in the literature, and is known to fail to reproduce the potential energy surface of He_3^+.[22,25] We also verify that the treatment fails when using accurate He_2^+ potentials, such as the *ab initio* results of Gadea *et al.*,[22] and accurate He_2 potentials, such as that given by Aziz.[21] Instead of the linear symmetric triatomic ion predicted by high level *ab initio* calculations, a linear ion with the charge localized on two atoms and a weakly bound third atom, $He–He_2^+$ is obtained. It is useful to understand the reasons for this failure.

The linear equilibrium structure of He_3^+, as opposed to an equilateral triangle, can be understood based on symmetry considerations. The deeply bound ground state potential of He_2^+ is the Σ_u state of odd symmetry, in which the wave function switches sign along the internuclear axis. The optimal configuration for the triatomic ion arises by maximizing this interaction. If atoms 1–2 and 2–3 are bound by Σ_u, then the 1–3 interaction must necessarily be Σ_g, which is strongly repulsive. This repulsion is minimized in the linear geometry. The DIM Hamiltonian yields a saddle point at $r_{12}=r_{23}=1.26$ Å, and the wave function at this point is given by the eigenvector $[-0.47, 0.72, -0.47]$, i.e., charge densities of 52% on the central atom and 22% on the terminal atoms. In the same region, the *ab initio* surface shows a minimum,[22] and the difference between the two ~ 0.2 eV, which is nearly 10% of the He_2^+ binding energy. This failure can arise from two sources; (1) The common assumption of total neglect of atomic overlap in the DIM Hamiltonian;[37] (2) extensive correlation energy at this configuration, which in DIM can be included by expanding the atomic bases to include excited state contributions. In order to pinpoint the

source of error we have performed the DIM treatment with the inclusion of overlap among ^1S basis functions. The overlap was estimated by assuming the Hartree–Fock electronic wave functions for each He atom and a single electronic orbital for He^+.[39] The overlap is significant ($\langle\phi_i|\phi_j\rangle \approx 0.3$ when $r_{ij}=1$ Å). Inclusion of this overlap lowers the DIM potential energy near the saddle point, however only by $\sim 200\ cm^{-1}$, far less than the sought discrepancy. Thus, we conclude that the failure is due to the absence of excited state configurations in the DIM matrix, to account for the extensive correlation energy observed in the *ab initio* analysis.[22] Despite the fact that these excited states lie some 20 eV above, at the relevant internuclear distances of ~ 1 Å, they must contribute to the binding of the ion. While such a treatment is feasible, it unnecessarily complicates the electronic Hamiltonian. Instead, in the semiempirical spirit of utility of DIM, we simply adjust the input pair parameters to reproduce the PES of the triatomic ion near its equilibrium geometry.

The required correction to the input potentials can be estimated directly. The DIM energy for the symmetric configuration, $r_{12}=r_{23}=r$, is given as

$$V(r)=\langle\psi|H|\psi\rangle=0.024V_{\Sigma_g(He_2^+)}(r)+0.732V_{\Sigma_u(He_2^+)}(r)+0.245V_{\Sigma(He_2)}(r) \tag{4}$$

which shows that the well at the equilibrium geometry of the ion arises from a cancellation between the large positive repulsive wall of He_2, at $r\sim 1.2$ Å, and the attractive part of the $He_2^+\ ^1\Sigma_u$ potential. Thus the experimental binding energy of -0.017 eV for the He_3^+ ion,[4] can be reproduced by artificially softening the well known repulsive wall of the He_2 potential.[18–21] A surface in good agreement with the *ab initio* results[22] is obtained when the repulsive wall of He_2 is lowered by 30% near $r=1$ Å. This correction, and the pair parameters used as input to the DIM Hamiltonian, are given in the Appendix. Note, an exact representation of the shallow bound region of the He_2 potential is not necessary for the dynamics at issue.

III. DYNAMICS

Mixed quantum/classical calculations are used to simulate the dynamics of the coupled electronic and nuclear coordinates. In the mean-field approach, the force is calculated from the average potential given by the expectation value of the electronic wavefunction, while in the surface hopping approach, where we use Tully's method of minimum hops,[35] the dynamics evolves on a single adiabatic PES. The calculation of the electronic wave function is the same in both methods. It is given by the time dependent Schrodinger equation in the adiabatic representation. The numerical algorithm solves for the coefficients a_i which are the expansion coefficients of the electronic wave function in the adiabatic basis set ψ_i multiplied by the phase factor that cancels fast oscillations

$$a_{ij}(t)=\langle\psi_i(t)|\Psi(t)\rangle e^{-(i/\hbar)\int_0^t V_t(\tau)d\tau}, \tag{5}$$

where $V_i(t)$ is the adiabatic potential energy of state i at a given nuclear configuration at time t. The Schrödinger equation for these coefficients is written as

$$\frac{da_i}{dt}=\sum_j d_{ij}a_j, \tag{6}$$

where d_{ij} is the nonadiabaticity matrix given as

$$d_{ij}=\langle\psi_i|\frac{\partial}{\partial t}|\psi_j\rangle. \tag{7}$$

In the actual algorithm matrix d_{ij} is expressed through the Hamiltonian matrix and its analytical derivatives with respect to coordinates. The details of the algorithm can be found in Ref. 34.

The nuclear dynamics is calculated by classical equations of motion. In the mean-field method, the force is obtained from the average potential,

$$F(t)=-\langle\Psi(t)|\frac{\partial H}{\partial r}|\Psi(t)\rangle. \tag{8}$$

This method gives consistent results that satisfy energy and momentum conservation, and a sensible approach to the calculation of the quantum subsystem when (a) the electronic density of states is large, (b) the adiabatic potential energy surfaces remain nearly parallel, (c) when changes in coordinates of the classical subsystem is not significant. However, the method does not predict correct long-time dynamics of the classical subsystem which becomes averaged over the different quantum channels. For example, the product of impact ionization of He_3 clusters can only be $He+He_2^+$, since the initial energy of the bound cluster necessarily lies below zero, and since the method maintains strict conservation of energy. Also the final state dynamics is unphysical since the He_2^+ fragment remains on a mixture of ground and excited states. Nevertheless, we use this method to simulate the initial electronic dynamics in the quantum clusters, namely the process of the hole hopping, to establish the relevant time scales for electronic and nuclear motions. The method is clearly appropriate at early times, before charge localization, when the dynamics occurs on several nearly parallel electronic surfaces.

In the surface-hopping dynamics, at any given time, the nuclear motion evolves on a single adiabatic surface. The probability of hopping from surface i to j at each time step is given by the rate of the density redistribution

$$P_{i\to j}(t)=\frac{2\Delta t\ \mathrm{Re}(a_j a_i^* d_{ji})}{a_i a_j^*}\ \theta(-\mathrm{Re}(a_j a_i^* d_{ji})), \tag{9}$$

where θ is the Heaviside function and Δt is the time step in which hops are allowed. After each hop the velocities of the heliums are adjusted to conserve total energy. The excess velocity is rescaled parallel to the vector,

$$\mathbf{h}_{ij}=\langle\psi_i|\frac{\partial}{\partial r}|\psi_j\rangle, \tag{10}$$

as described by Herman.[40] The hop is not allowed if it requires kinetic energy greater than available in the degree of freedom parallel to $\mathbf{h}_{ij}$.

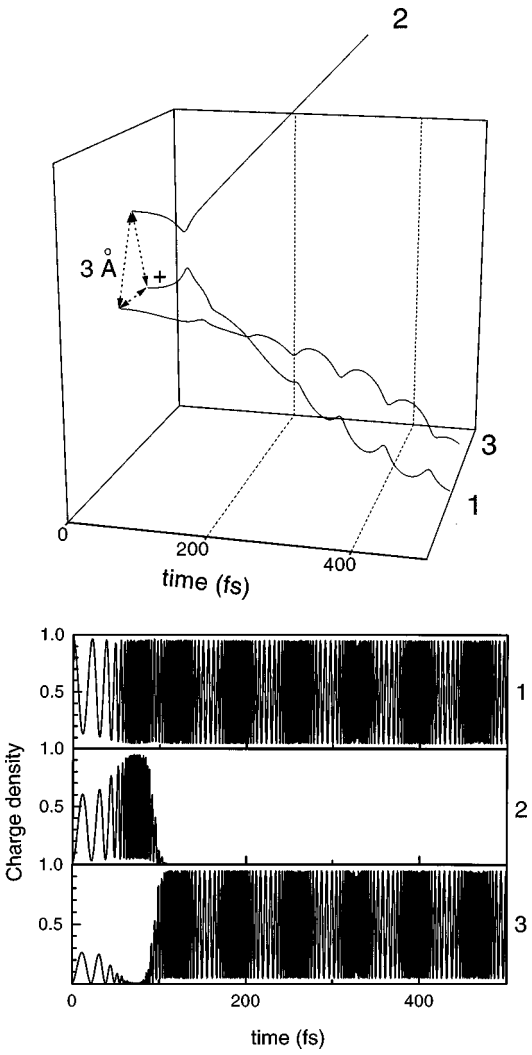

FIG. 1. Mean-field dynamics of a He_3^+ cluster, with initial internuclear separations of 3 Å. (a) Nuclear trajectories, (b) hole density on each atom. Initially, the hole is on atom 1, it delocalizes to all three within 20 fs, then traps on the 1–2 pair near $t \sim 70$ fs, and finally, it hops to the 1–3 pair with the ejection of atom 2.

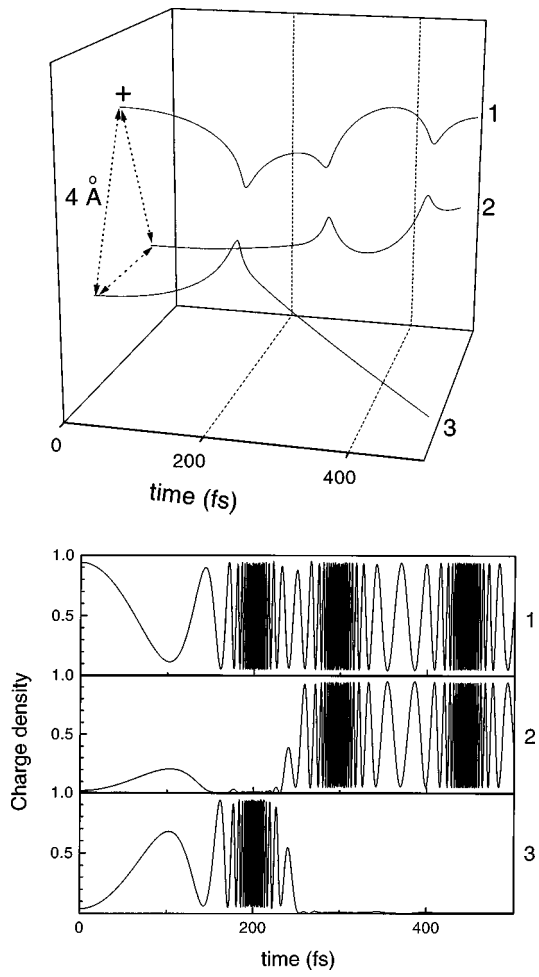

FIG. 2. Mean-field dynamics of a He_3^+ cluster, with initial internuclear separations of 4 Å. (a) Nuclear trajectories, (b) hole density on each atom. Initially, the hole is on atom 1, it delocalizes to all three at $t \sim 100$ fs, then traps on the 1–3 pair for one vibrational period ($t = 150$–250 fs), the charge hops to the 1–2 pair with the ejection of atom 3.

IV. RESULTS AND DISCUSSION

A. Mean field dynamics

We first investigate the dynamics of clusters using the mean-field method. As already mentioned, the method gives unphysical dynamics when the electronic states are well separated. However, the initial dynamics is determined mostly by hole delocalization and the nuclear evolution on nearly parallel closely lying set of the PES (in the limit of large clusters these constitute the conduction band of the hole). The mean-field approach preserves the coherence of the quantum subsystem and gives a consistent treatment for the hole dynamics.

Figures 1 and 2 summarize the He_3^+ dynamics subject to two different initial conditions. In each case, the motion of nuclear coordinates is shown in the plane of the system in a 3D plot, and the time dependent charge density on each atom is given underneath. In Fig. 1, the atoms are initially positioned at the vertices of an equilateral triangle with 3 Å sides and displaced from these positions in random directions by 0.1 Å. This brakes the symmetry of the system, and facilitates meaningful dynamics (in mean-field, in a perfectly symmetric cluster, the system will execute symmetric breathing vibrations, with no further dynamics). Figure 1(b) shows that the charge starts on atom 1, within 10 fs it delocalizes over all three atoms, and subsequently oscillates between pairs with a period determined by the pair internuclear separation. After about 70 fs the charge localizes on the 1–2 pair. The contraction of this bond is marked by the high frequency charge oscillations on atoms 1 and 2, near $t = 100$ fs. During the outbound stretch of the 1–2 bond, the charge hops to the 1–3 pair, and atom 2 is ejected as a neutral. The electronic energy of the 1–2 pair, is converted into translational energy of departing atom 2. The dynamics is complete after about 120 fs with the formation of $He + He_2^+$. Now, the charge oscillates between atoms 1 and 3 with a frequency given by the exchange energy of the diatomic ion, $1/\tau = (V(\Sigma_g) - V(\Sigma_u))/2\hbar$, which in turn is determined by the internuclear separation. Note, the frequency of the He_2^+ vibrations correspond to motion on the mean potential, $V = (V(\Sigma_g) - V(\Sigma_u))/2$, which is orders of magnitude less than the real frequency on the Σ_u potential. Figure 2 illustrates the dy-

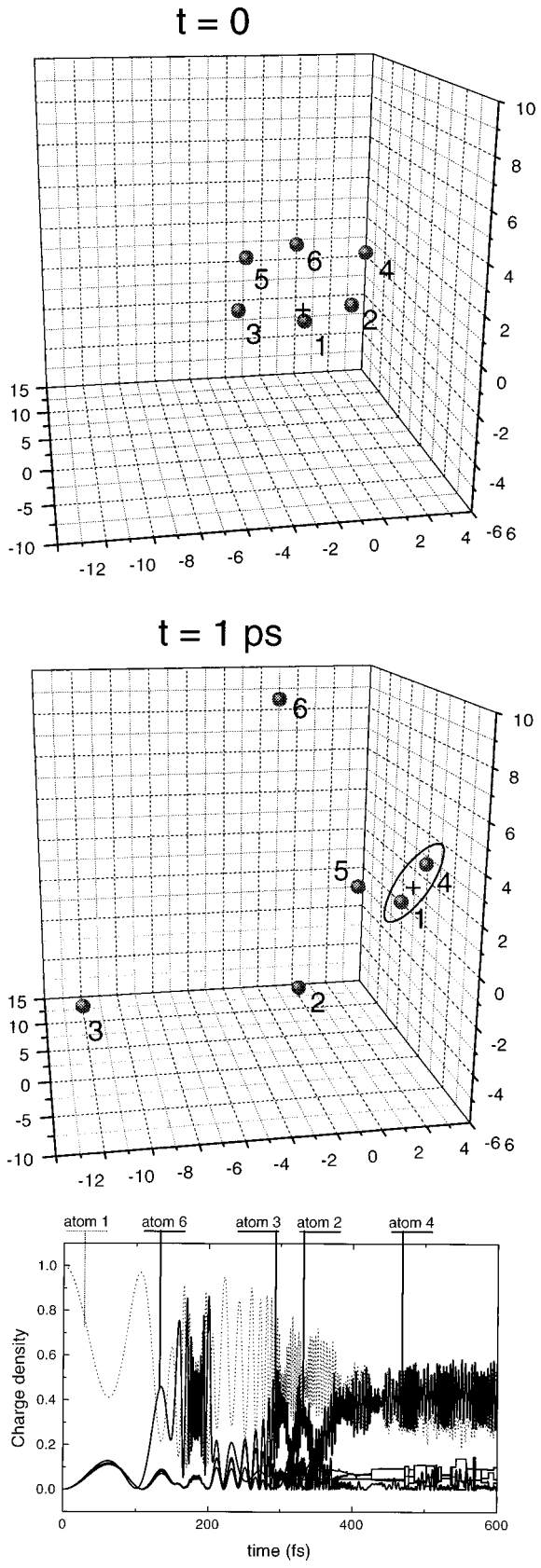

FIG. 3. Mean-field dynamics of a He_6^+ cluster. (a) Snapshots of the cluster structure at $t=0$, and at $t=1$ ps; (b) hole densities on individual atoms. The ejection of neutrals, atoms 6, 3, and 2 in sequence, is controlled by the mechanism of hole localization on pairs (1–6, 1–3, 1–2, 1–4), and subsequent simultaneous hole-hop and ejection. The 1–4 pair forms the final He_2^+.

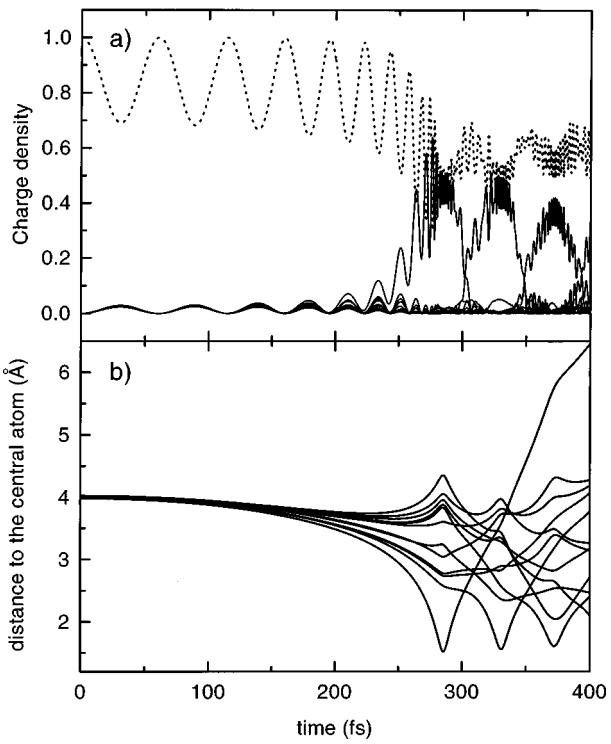

FIG. 4. Mean-field dynamics of a He_{13}^+ cluster. (a) Hole density on each atom; (b) nuclear trajectories, as distance from the central atom. The sequential ejection of atoms follows the pattern observed in the smaller clusters.

namics of the triatomic ion starting with an internuclear separation of 4 Å. Qualitatively, the process is the same, however, the relevant time scales are quite different. The period of surface hopping is now ~100 fs, and the time for the first collision (localization of the charge to a pair) takes place after 200 fs. The dynamics is complete after 300 fs when atom 3 escapes as the charge hops to the 1–2 pair to form the He_2^+.

The results of a similar calculation for H_6^+ are summarized in Fig. 3. The interatomic separations at $t=0$ is taken as 4 Å. The dynamics involves an initial charge redistribution from atom 1 to the rest within ~50 fs. This is followed by localization of the charge on the 1–6 pair, for the period between $t=150-200$ fs. Atom 6 escapes on the outbound stretch, as the charge delocalizes over the remaining cluster. This is followed by consecutive hops of the charge on pairs 1–3, 1–2, and 1–4. The 1–4 pair forms the final He_2^+. Figure 3(a) shows two snapshots of the system at $t=0$ and at $t=1$ ps. Atoms 6, 2, and 3, which were consecutively involved in the formation of the diatomic ion, have consecutively escaped the cluster. Quite clearly, the mechanism of ejection of fast neutrals from the larger cluster is a repeat of the charge localization and ejection during the outbound stretch of the diatomic ion that was observed in the case of the triatomic clusters.

The same pattern is observed in the larger clusters, as illustrated for the case of He_{13}^+ in Fig. 4. The top panel shows the distances of the peripheral atoms from the central atom. The bottom panel shows the charge density on each atom. Initially, the atoms are positioned at the perfect single shell structure with interatomic distances of 4 Å. Then the sym-

metry is broken by random displacement of the atoms by 0.1 Å. The charge is localized on the central atom at $t=0$. In the first 200 fs the delocalization of charge is observed as oscillations of density between the central atom and the shell of the cluster. As the cluster contracts by polarization forces, the charge amplitude on the peripheral atoms grows, and the charge oscillation frequency increases. After about 250 fs the symmetry of this breathing motion breaks as one of the shell atoms comes closer to the center. This atom is further accelerated toward the center by charge localization to form the diatomic ion. As in the smaller clusters, the kinetic energy of the He_2^+ is too high and on its outbound stretch the atom escapes with a simultaneous hop of the charge to a second member of the shell atoms. This process repeats with ~ 100 fs intervals, as the cluster breaks up by consecutively ejecting fast He neutrals. The final product is again a bare He_2^+, and 11 He neutrals.

The above establish the dependence of hole hopping times on internuclear separations and give a qualitative description of the governing dynamics at early times. Among these the notable features are

(a) A hole created on a single atom will delocalize over the cluster on time scales of 10–200 fs, depending on the initial internuclear separation, this process is usually faster than any significant nuclear motions. In mean-field, in large clusters, the hole will migrate to the central atom to optimize polarization forces.

(b) The process of charge localization on a pair occurs as one of the interatomic distances shrinks significantly in comparison to the others. In a perfectly symmetric cluster the charge will delocalize and breadth as the cluster breadths, and in mean-field, no fragmentation can occur.

(c) Charge localization on a pair occurs with positive feedback between nuclear and electronic coordinates, therefore, small fluctuations in the symmetry of the cluster determines the direction of motion of the charge.

(d) The localized charge hops during the outbound stretch of the initial diatomic ion, in a process that can be described as that of the triatomic unit,

$$He_2^+(v)+He \rightarrow He(T)+He_2^+(T',v'<v)$$

in this process, the vibrational energy v of the reagent He_2^+ is converted to relative translational energy of the product. The kinetic energy, T, leads to ejection of fast neutral atoms while T' leads to ejection of the diatomic ion from the cluster.

Several important features of the dynamics are incorrect due to the averaging intrinsic in mean-field. First, it is clear that the frequencies of the He_2^+ molecules formed during the dynamics are not physical, since they result from the mixture of Σ_u and Σ_g states. Since the kinetic energy of the system is conserved, an incorrect internal energy of the ionic fragment in turn implies that the translational energy of the ejected fragments is incorrect. Second, mean-field dynamics cannot lead to complete dissociation of the cluster, $He_n \rightarrow (n-1)He+He^+$, a channel observed in experiments.[5] This is simply a consequence of the strict energy conservation of the method and the fact that we start at a total energy below zero. In practice, the initial energy of the excited electronic state can be above zero, which can lead to complete dissociation after adiabatic propagation on this surface. To develop the systematics of final channels, we carry out the surface hopping algorithm starting with proper initial conditions and using an ensemble of trajectories.

B. Surface hopping dynamics

The validity of classical dynamics in describing the nuclear coordinates for particles as light as He is always questionable. Such an approach would be completely inappropriate for the case of the neutral species. However, since the introduction of the positive charge in the system changes the scale of the potential energy by 3 orders of magnitude, classical representations with proper statistics become acceptable. Nevertheless, since the relevant initial distribution of atomic positions and momenta are those of the neutral clusters, they reflect diffuse distributions of the quantum cluster that must be appropriately sampled. We have seen in the previous section that for average interatomic separations of 3–4 Å, charge transfer occurs on the time scale of 10–100 fs. In He clusters of the size range considered here, depending on the size of the cluster, the average interatomic separations range between 3 Å and 10 Å, with a large dispersion about these values. Accordingly, the initial charge transfer probabilities range from 10 fs to 1 ps, and when properly weighted will be dominated by the shorter time hops. This consideration is the basis for the hopping kinetics devised by Halberstadt and Janda.[12]

Initial conditions of the He_3 cluster are derived from the variational quantum Monte Carlo wave function, which is given in the form a product of pair functions in Ref. 32,

$$\psi(r_1,r_2,r_3)=\psi_0(r_{12})\psi_0(r_{23})\psi_0(r_{13}). \tag{11}$$

We use a Monte Carlo sampling algorithm to select initial positions from the $|\psi|^2$ of this distribution. Random initial momenta are sampled from a Gaussian distribution with a spread of $\hbar/\Delta x$ where $\Delta x \sim 2$ Å, which is roughly the spatial spread of the wave function. Approximations in the momentum distribution are permissible since they have little effect on the dynamics. In fact the initial kinetic energy of the nuclei is of order of 1 cm^{-1} while the potential energy of the system upon the introduction of the positive charge is in the range 50–300 cm^{-1}. With initial positions and momenta defined, we ionize a single He atom and start the propagation. The initial electronic wave function is expanded in the adiabatic basis and the initial surface for the propagation is determined randomly. The wave function is reset to $a_k=1$ for the propagation surface k and $a_i=0$ for $i \neq k$.

1. He_3^+

A set of 50 trajectories were propagated for 6 ps to simulate the dynamics of the He_3^+ cluster. Representative trajectories are illustrated in Fig. 5, 6, and 7, along with the adiabatic energies of the system as a function of time. The bold line indicates the potential energy surface on which the dynamics evolves.

The trajectories in Fig. 5 and 6 start with negative initial energy, and are therefore destined to form $He+He_2^+$. The dynamics of the charge localization and the formation of

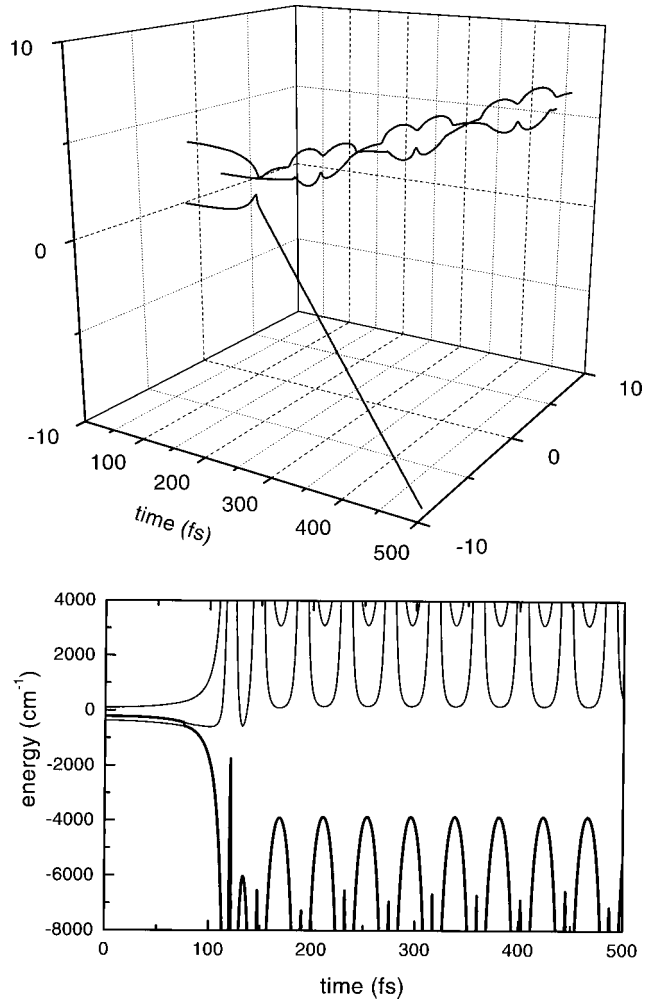

FIG. 5. Surface hopping dynamics of $He_3^+ \rightarrow He + He_2^+$. (a) Trajectory, (b) potential energies, with the surface of evolution indicated in bold. The hop to the lowest energy surface of the triatomic occurs at $t \sim 80$ fs, the triatomic then dissociates to form $He + He_2^+$ with $\sim 4000\ cm^{-1}$ of vibrational energy converted to translation.

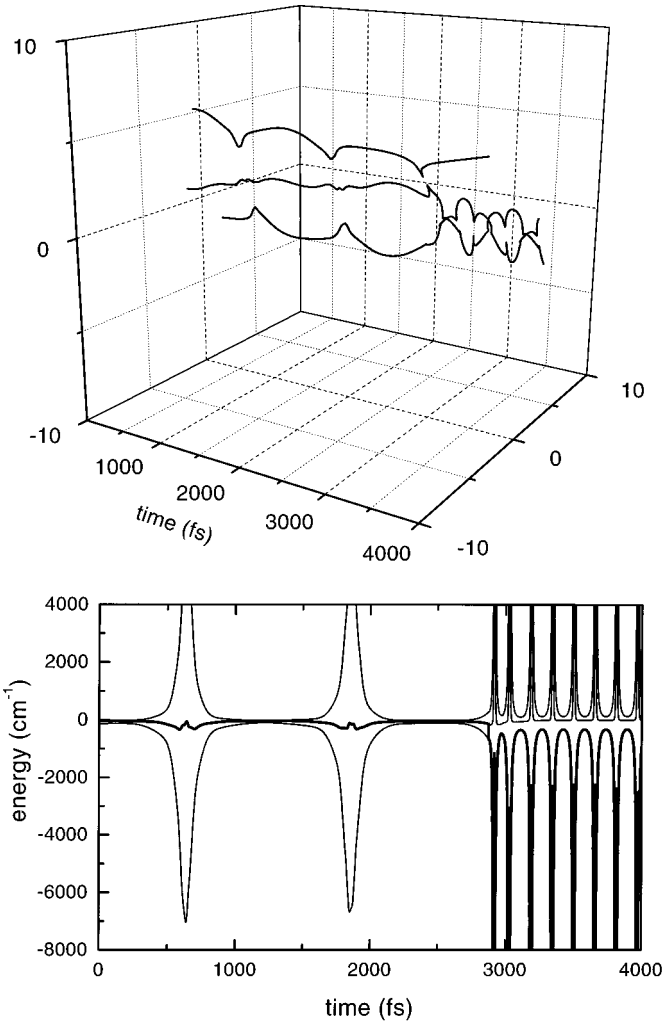

FIG. 6. Surface hopping dynamics of $He_3^+ \rightarrow He + He_2^+$. Despite several curve crossing opportunities, the system remains on the excited adiabatic surface for ~ 3 ps. Once the hop occurs, the cluster dissociates with $\sim 300\ cm^{-1}$ converted from vibration to translation.

He_2^+ is determined mostly by the adiabatic surface on which the system starts. The time scale is determined by the time at which the system hops onto the lowest potential surface and lies in the range of 0–5 ps. After this hop the dynamics is very similar in all trajectories and the formation of a stable molecule occurs on the time scale of hundreds of femtoseconds. In the trajectory of Fig. 5, the system starts on the excited ionic surface, the triatomic executes two symmetric bond compressions, but the charge remains delocalized. The third bond compression is asymmetric leading to the nonadiabatic transition and localization of the charge on one pair. As before, this is followed by the break-up of the pair, with a simultaneous adiabatic charge hop to the second pair and localizes on the lowest PES, at $t \sim 3$ ps, permanently forming $He + He_2^+$. This general process can be visualized by considering the motion over the contour plots shown in Fig. 8. Upon the adiabatic hop to the lowest energy surface, the vibrational energy in the entrance channel corresponding to charge localization on the 1–2 pair, is sufficient to turn the corner, to exit as the 2–3 pair by the ejection of atom 1 as a neutral. Since this adiabatic reaction of charge hopping, which corresponds to going from the entrance valley to the exit valley, has no barrier, the fragmentation of the triatomic will always involve charge hopping. This is also the mechanism for converting vibrational energy of the initial diatomic ion to translational energy between the departing final molecular ion and neutral atom.

The same general principles are observed in the trajectories of Fig. 6. Now, the lowest surface is accessed upon the first bond compression, at $t \sim 100$ fs, and again the first pair to which the charge hops dissociates, and the final molecular ion is the second pair. In this case, the vibrational energy loss is significantly higher than in the case of the trajectory shown in Fig. 5. The product molecular ion is formed at $\sim 4000\ cm^{-1}$ below its dissociation energy, at $t \sim 150$ fs. This vibrational energy is impulsively transferred to relative translation of fragments.

Some of the trajectories start on a PES of positive energy, as in the case illustrated in Fig. 7. In all such realizations, the cluster is observed to break-up into strictly atomic fragments, although the process whereby the He_2^+ is stabilized by transferring the initial excess energy to translation of

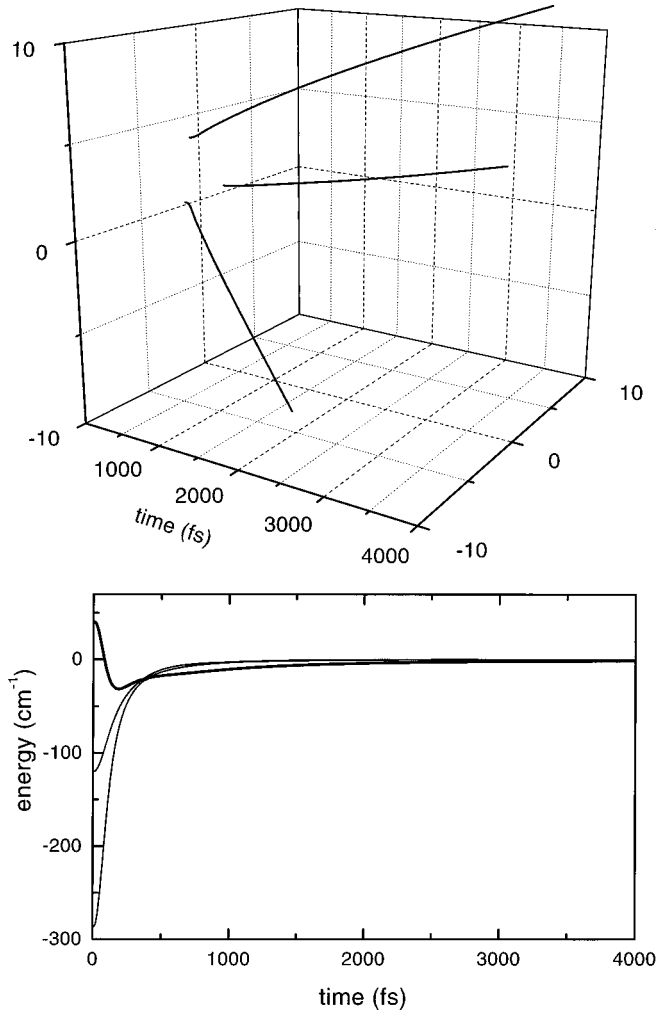

FIG. 7. Surface hopping dynamics of $He_3^+ \rightarrow He+He+He^+$.

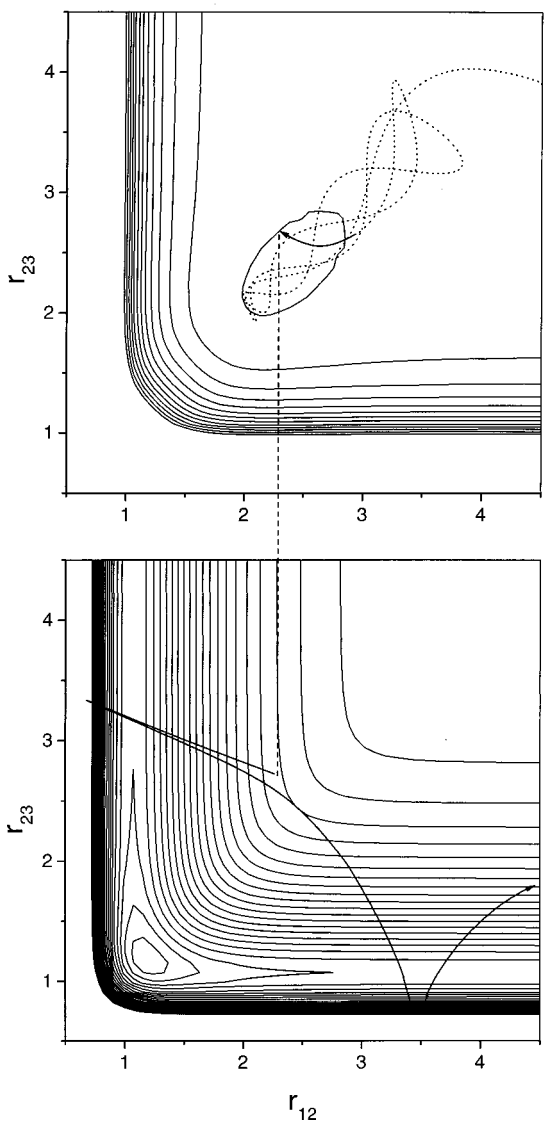

FIG. 8. Surface hopping dynamics of He_3^+ illustrating the general mechanism of fragmentation, which can be understood in terms of the adiabatic collinear triatomic surfaces.

the neutral atom is in principle possible (all trajectories that start on a PES with negative energy, must lead to formation of the diatomic ion). If we assume that all trajectories that start on a PES of positive energy are destined to form the atomic products, the branching ratio for fragmentation into $He+He+He^+$ and $He+He_2^+$ channels can be obtained from initial conditions alone. We determine this branching ratio based on a sampling of 2000 initial conditions. If we assume that the hole is initially localized on a single atom, then the atomic channel constitutes $20\pm0.5\%$ of the ensemble. If we assume that the initial hole function is a randomly chosen eigenstate of the cluster, as had been done in simulations of Ar_n^+ clusters,[28] then this channel constitutes $22\pm0.5\%$ of the ensemble. These results are very different from the recent experimental determination of this branching ratio, where using a diffraction grating the neutrals are separated and ionized.[5] The deduced branching ratio in the experiments is a function of expansion temperature, and tends to 55% at the lowest temperature.[5] The origin of this wide discrepancy, and the observed source temperature dependence in the experiment, is not clear. Independent of any computational details this branching ratio cannot exceed 33%. This ratio would be obtained if for all configurations of the neutral cluster there were one vertically accessible positive PES, and that all realizations of this state lead to fragmentation into atomic products. Yet, at the large internuclear distances characteristic of the neutral cluster, due to polarization interactions, all three of the PESs of the triatomic ion are bound with respect to the $He+He+He^+$ asymptote, and therefore the probability of attaining an initial positive energy is significantly smaller than 33%. An experimental finding greater than this fraction may be indicative of the participation of higher excited electronic states, a consideration that can be verified by testing the voltage dependence of the branching ratio.

2. He_{13}^+

Realistic initial conditions for the quantum He_{13} cluster are generated using the average size of the cluster obtained from QMC calculations.[31,33] The shell atoms are positioned equidistantly from the center in order to generate a cluster of

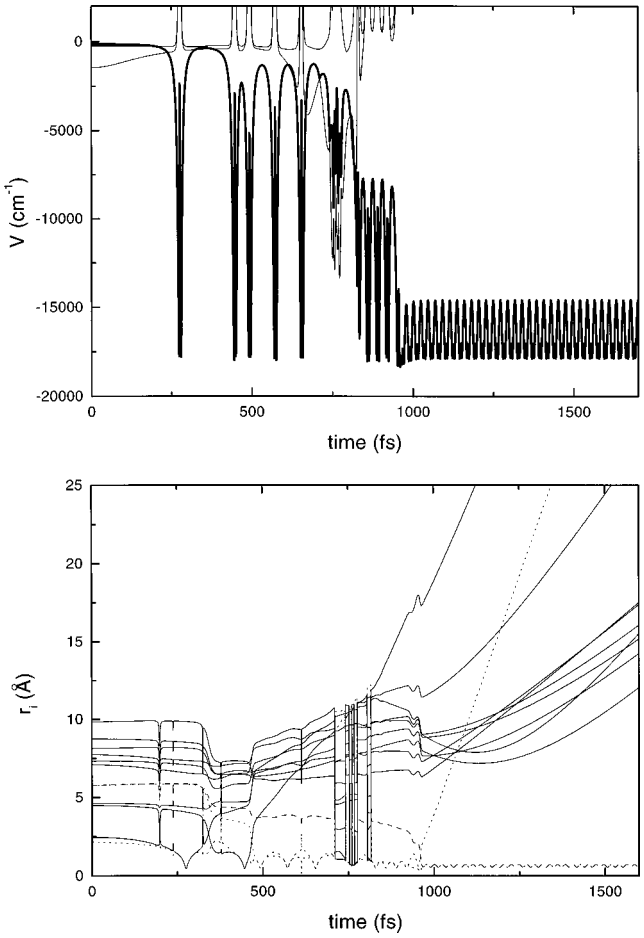

FIG. 9. Surface hopping dynamics of He_{13}^+. (a) Three of the adiabatic potential energy surfaces involved in the dynamics. (b) Atomic separations from the center of charge.

16 Å diameter. We then misplace the atoms from their original position with a Gaussian probability of full width at half maximum of 3.6 Å.

In Fig. 9 we show the evolution on the adiabatic PES for 4 ps. Only three of the thirteen surfaces are shown for clarity, and as before the bold line indicates the PES of evolution. The trajectories in this case are plots of the atomic distances from the ''center-of-mass'' of the charge. Accordingly, when the charge localizes on a pair, two distances will be short while the others remain significantly larger. The trajectory has clear discontinuities when surface hopping occurs, since at these instances the electronic wavefunction, and hence the charge density, changes suddenly.

We follow the history of this representative cluster, then draw some generalizations. The trajectory starts on the highest of the shown surfaces, and the charge is mainly on the 1–2 pair of peripheral atoms. In contrast with the mean-field treatment, the charge does not move to the center of the cluster, where it would be at a lower energy. The entire cluster starts compressing. At $t \sim 200$ fs, the charge hops to the 1–3 pair which is accelerated to reach the He_2^+ repulsive wall at $t = 275$ fs. During the stretch of the 1–3 bond, the charge hops back to the 1–2 pair and atom 3 is ejected as a neutral. The 1–2 bond follows the same fate, after a full bond compression, atom 2 is ejected as a neutral while atom 5 is accelerated toward the charge to form the 1–5 diatomic ion, this pair undergoes two vibrational oscillations on the lowest PES. The ejected atoms 2 and 3 collide with the cluster. The colliding neutrals lower the excited state, to create degeneracies (crossings) with the lowest surface. This allows the charge to resonantly hop between pairs during $t = 700$ fs and 800 fs. With a final $v-T$ transfer, atom 3 escapes the cluster, while the 1–5 diatomic ion reforms some 7000 cm^{-1} below dissociation energy. The adiabatic charge exchange illustrated in Fig. 8 occurs at $t \sim 900$ fs, where the 1–5 ion dissociates to form the final product diatomic ion as the 5–6 pair. Atom 1 is ejected as a fast neutral, and the 5–6 pair recoils as He_2^+ from a relatively hot cluster containing 7 atoms. The neutral cluster of seven-atoms has sufficient energy to eventually dissociate into atoms. However, it is important to note that the molecular ion is ejected from the cluster prior to its break-up, as opposed to shedding neutrals by evaporation. Note that the ejected molecular ion contains only ~ 3000 cm^{-1} in internal energy, which corresponds to ~ 2 vibrational quanta. During the 1 ps of dynamics, the ionic cluster converts $\sim 15\,000$ cm^{-1} of vibrational energy into translation of the fragments.

The relevant dynamics of large cluster ions can be separated into two histories; propagation on excited surfaces with hole hopping, and hole localization by trapping on the ground PES and subsequent adiabatic evolution. These two segments of evolution are separated by the nonadiabatic transfer to the lowest PES. Both adiabatic and nonadiabatic hole hopping is accompanied by vibrational energy loss at the ionic center, therefore trapping, and ejection of neutrals. A crucial consideration in the understanding of this process is the recognition that the charge is localized on no more than 3 atoms at one time. The sequence of processes can then be broken down into individual steps involving triatomics. The exception to this is the process of resonant energy hop between different pairs. As illustrated in the trajectory of Fig. 9, this can occur when the charge is localized on a pair and a nearby pair of neutrals undergo a high energy collision. The latter provides the proper nuclear Franck–Condon factor for the charge to detrap. Such correlated hops are limited to early times and do not lead to extensive migration of charge. The hole hopping and self-trapping in the bulk should also be possible to understand by considering three atoms at a time. We may then expect complete vibrational relaxation to form the stable He_3^+ as the positive ion core. Once the charge localization starts, only several hole hops accompanied by $v-T$ transfer in head-on collisions between He and He_2^+ are required to accomplish this. Accordingly, we may estimate that the ion will reach $v = 0$ in its symmetric well within $t \sim 5$ ps. Note, in the case of small clusters, ejection of He_2^+ will pre-empt completion of vibrational relaxation. Only in very large clusters will there be a finite chance of trapping the fully relaxed triatomic ion, bare or weakly solvated by neutrals, a finding which is quite consistent with experiments.[13]

V. CONCLUSIONS

We have presented simulations of dynamics in small He cluster ions in an attempt to provide a detailed picture of the

elementary steps involved in hole migration, self-trapping, and fragmentation of clusters. The operative mechanism, dominated by dynamics of triatomic units, emerges as a building block for reconstructing the same events in the larger clusters and in the bulk. Several important conclusions deserve reiteration.

The sudden removal of an electron from a single He atom leads to a hole that immediately ($t=10-100$ fs) delocalizes over several. The migration of such a hole is dictated by the contraction of an internuclear distance, and is subject to positive feedback (as the hole localizes on a pair, they are accelerated toward each other). Only in mean-field, which may be considered as appropriate for very large clusters, does the hole feel the polarization bias to migrate to the center of the cluster. In smaller clusters, this bias can be overridden by adiabatic migration on an excited electronic surface. Once a nonadiabatic transfer occurs to the lowest electronic surface occurs, self-trapping is initiated, and although the charge may hop between pairs due to degeneracies created by head-on collisions of fast neutrals, the extensive $v-T$ transfer processes ascertain that this process is not reversible. The adiabatic hole hops on both excited and ground electronic surfaces occurs in triatomic units, and is accompanied by extensive $v-T$ transfer. This in turn insures that in small clusters the diatomic ion will be ejected from the cluster, as opposed to cooling by sequential evaporation of neutrals. Given this highly localized dynamics, it should be possible to simulate the process in extended systems, in large clusters and in the bulk.

The mechanism of violent ejection of diatomic ions from the cluster is consistent with experiments, where the predominance of He_2^+ in electron impact ionization of very large clusters has been noted to be inconsistent with the picture of evaporative cooling.[13] In the case of electron impact ionization of He_3 clusters, our findings are in conflict with experiments.[5] We determine a branching fraction for the $He+He+He^+$ channel of 20%, to be contrasted with the experimental determination of $\sim 55\%$. In the absence of involvement of electronic states that correlate with the excited atoms, this branching ratio is determined by the Franck–Condon projection of the neutral wave function on the ionic surfaces, and cannot exceed 33%. The experimental result is therefore indicative of the participation of excited electronic states in the ionization process. Finally, in the absence of the possibility of ejection, in the bulk or in very large He droplets, the ionic center will fully relax vibrationally to form the triatomic as the ionic core. This has already been verified in photoabsorption measurements in size selected clusters, in which it has been shown that the absorption maxima undergo a relatively small red shift from He_3^+ at 5.34 eV to He_{30}^+ at 4.98 eV,[7] while the vertical absorption of He is at ~ 10 eV.[22–24] The same diagnosis should be possible in the bulk, where we estimate a formation time scale for the ground state ion to be ~ 5 ps.

ACKNOWLEDGMENTS

This work was supported in part by the AFOSR, under a University Research Initiative Grant No. F49620-1-0251, and in part by the NSF under Grant No. CHE-9708382.

TABLE I. Parameters used to describe pair potentials according to Eqs. (A1), and (A2). (distances in Å, and energies in cm^{-1}).

	He–He original	He–He adjusted	He–He^+, Σ_g	He–He^+, Σ_u
β	6.282	4.4965	2.8858	2.9055
n_{-2}	0,	−728902	202740	454087
n_{-1}	464359	3615195	−81909	−805999
n_0	972756	−1411451	2434348	2434348
n_1	−102225	−2241850	−1662080	−1851016
n_2	−8442915	2665155	777029	269630
n_3	−419755	−370440	−62492	−55753
n_4	7606138	0	0	0
α	0	0	12100	12100

APPENDIX

The functional form used for fitting the He_2 potential,

$$V(r)=e^{-\beta r}\sum_{n=-2}^{4} a_n r^n \tag{A1}$$

was originally proposed by Ceperly and Partridge,[20] who used a quantum Monte Carlo calculation to determine the He–He potential at short distances, between 0.5 Å and 1.8 Å. This range of the potential is rather well characterized,[18,19] and analyzed since.[21] Using the best accepted forms, does not allow the construction of a reliable surface using a minimal basis DIM Hamiltonian. This failure has already been documented in the literature.[22,25] As discussed in the text, we adjust the repulsive wall of the He–He interaction to generate a He_3^+ surface that agrees with the ab initio results. Adjusted potential is obtained by changing the slope of the repulsive wall and then performing a nonlinear fit to the form (A1). These parameters are summarized in Table I.

For the ionic He_2^+ potential, we have used an additional term corresponding to the polarizability (see Fig. 10),

$$V(r)=e^{-\beta r}\sum_{n=-2}^{4} a_n r^n-\alpha/r^4. \tag{A2}$$

The Σ_g and Σ_u potentials of He_2^+ are the fits of the points given by Gadea and Pidarova.[22] The parameters used are collected in Table I.

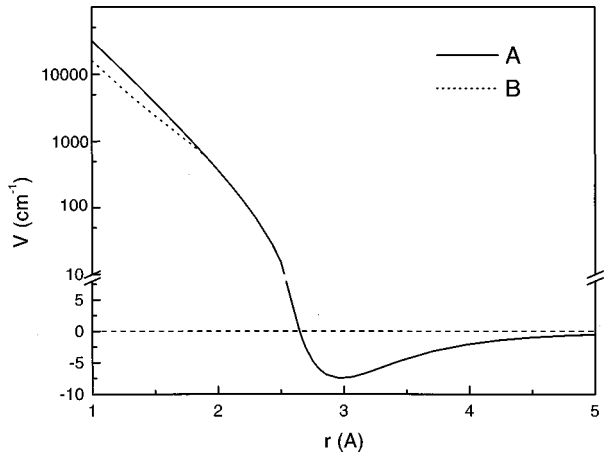

FIG. 10. The He_2 pair potential (solid line) and the adjusted potential (dashed line).

[1] K. B. Whaley, *Spectroscopy and Microscopic Theory of Doped Helium Clusters* in *Advances in Molecular Vibrations and Collision Dynamics*, edited by J. Bowman (JAI, New York, 1998), Vol. III.
[2] E. W. Becker, R. Klingelhofer, and P. Lohse, Z. Naturforsch. A **16**, 1259 (1961).
[3] J. G. Maas, N. P. Van Asselt, P. J. Nowak, J. Los, S. D. Peyeremhoff, and R. J. Bunker, Chem. Phys. **17**, 217 (1976).
[4] P. L. Patterson, J. Chem. Phys. **48**, 3625 (1968).
[5] W. Schlöllkopf and J. P. Toennies, J. Chem. Phys. **104**, 1155 (1996).
[6] (a) H. Buchenau, E. L. Knuth, J. Northby, J. P. Toennies, and C. Winkler, J. Chem. Phys. **92**, 6875 (1990); (b) H. Buchenau, J. P. Toennies, and J. A. Northby, *ibid.* **95**, 8134 (1991).
[7] (a) P. W. Stephans and J. G. King, Phys. Rev. Lett. **51**, 1538 (1983); (b) T. M. Kojima, N. Kobayashi, and Y. Kaneko, Z. Phys. D **22**, 645 (1992).
[8] (a) B. von Issendorff, H. Haberland, R. Frochtenicht, and J. P. Toennies, Chem. Phys. Lett. **233**, 23 (1995); (b) H. Haberland, B. von Issendorff, R. Frochtenicht, and J. P. Toennies, J. Chem. Phys. **102**, 8773 (1995).
[9] A. Scheidemann, B. Schilling, and J. P. Toennies, J. Phys. Chem. **97**, 2128 (1993).
[10] M. Lewrenz, B. Schilling, and J. P. Toennies, J. Chem. Phys. **102**, 8191 (1995).
[11] B. E. Callicoat, D. D. Mar, V. A. Apkarian, and K. C. Janda, J. Chem. Phys. **105**, 7872 (1996).
[12] N. Halberstadt and K. C. Janda, Chem. Phys. Lett. **282**, 409 (1998).
[13] (a) M. Lewrenz, B. Schilling, and J. P. Toennies, Chem. Phys. Lett. **206**, 381 (1993); (b) B. E. Callicoat, Ph.D. thesis, University of California, Irvine, 1998.
[14] B. E. Callicoatt, K. Forde, T. Ruchti, L. Jung, K. C. Janda, and N. Halberstadt, J. Chem. Phys. (submitted).
[15] K. R. Atkins, in *Proceedings of the International School of Physics Enrico Fermi, Course XXI on Liquid Helium*, edited by G. Careri Ed. (Academic, New York, 1963), p. 403.
[16] L. Meyer and F. Reif, Phys. Rev. **110**, 279 (1958).
[17] A. Benderskii, R. Zadoyan, N. Schwentner, and V. A. Apkarian, SPIE Proc. **42**, 3273 (1998).
[18] K. T. Tang and J. P. Toennies, Z. Phys. D **1**, 91 (1986).
[19] D. E. Nitz, D. Sieglaff, M. Lagus, E. Abraham, P. Wold, and K. Swanson, Phys. Rev. A **47**, 3861 (1993).
[20] D. M. Ceperley and H. Partridge, J. Chem. Phys. **84**, 820 (1986).
[21] R. A. Aziz, A. Krantz, and M. J. Slaman, Z. Phys. D **21**, 251 (1991); R. A. Aziz, and M. J. Slaman, Metrologia **27**, 211 (1990); Z. Phys. D **25**, 343 (1993).
[22] F. G. Gadea, and I. Paidarova, Chem. Phys. **209**, 281 (1996).
[23] J. Ackermann and H. Hogreve, Chem. Phys. **157**, 75 (1991).
[24] (a) M. Rosi and C. W. Bauschlicher, Chem. Phys. Lett. **159**, 479 (1989); (b) V. Steamler, Z. Phys. D **16**, 219 (1990); **22**, 741 (1990).
[25] F. Y. Naumkin, P. J. Knowles, and J. N. Murrell, Chem. Phys. **193**, 27 (1995).
[26] M. Amarouche, F. X. Gadea, and J. Durup, Chem. Phys. **130**, 145 (1989).
[27] I. Last and T. F. George, J. Chem. Phys. **93**, 8925 (1990); Chem. Phys. Lett. **183**, 547 (1991); J. Chem. Phys. **98**, 6406 (1993); A. Goldberg, I. Last, and T. F. George, *ibid.* **100**, 8277 (1994).
[28] A. Bastida, N. Halberstadt, J. A. Beswick, F. X. Gadea, U. Buck, R. Galonska, and C. Lauenstein, Chem. Phys. Lett. **249**, 1 (1996).
[29] P. J. Kuntz and J. Valldorf, Z. Phys. D **8**, 195 (1988).
[30] T. Ikegami, T. Kondow, and S. Iwata, J. Chem. Phys. **98**, 3038 (1993).
[31] M. Lewerenz, J. Chem. Phys. **106**, 4596 (1997).
[32] S. W. Rick, D. L. Lynch, and J. D. Doll, J. Chem. Phys. **95**, 3506 (1991).
[33] M. V. Rama Krishna, and K. B. Whaley, J. Chem. Phys. **93**, 6738 (1990).
[34] D. F. Coker, in *Computer Simulation in Chemical Physics*, edited by M. P. Allen and D. J. Tildesley (Kluwer, Amsterdam, 1993).
[35] J. C. Tully, J. Chem. Phys. **93**, 1061 (1990).
[36] F. O. Ellison, J. Am. Chem. Soc. **85**, 3540 (1963).
[37] J. C. Tully, in *Modern Theoretical Chemistry, Semiempirical Methods of Electronic Structure Calculations*, edited by G. A. Segal (Plenum, New York, 1977), Vol. 7A, Chap. 6; J. C. Tully, in *Potential Energy Surfaces*, edited by K. P. Lawley (Wiley, New York, 1980), pp. 63–112.
[38] (a) P. J. Kuntz, in *Dynamics of Molecular Collisions*, edited by W. H. Miller (Plenum, New York, 1976), Part B, p. 53; (b) P. J. Kuntz, in *Atom-Molecule Collision Theory—A Guide for the Experimentalist*, edited by R. B. Bernstein (Plenum, New York, 1979), Chap. 3; (c) P. J. Kuntz, in *Theoretical Models of Chemical Bonding, Part 2, The Concept of the Chemical Bond*, edited by Z. B. Maksic (Springer, Berlin, 1980), pp. 321–376.
[39] A. A. Radzig and B. M. Smirnov, *Reference Data on Atoms, Molecules, and Ions*, Springer Series in Chemical Physics (Springer, New York, 1985), Vol. 31.
[40] M. F. Herman, J. Chem. Phys. **81**, 754 (1984); **81**, 764 (1984).